



Interleukin-4 improves white matter integrity and functional recovery after murine traumatic brain injury via oligodendroglial PPAR γ

Hongjian Pu^{1,2,*} , Xuan Zheng^{2,*}, Xiaoyan Jiang^{1,2,*},
Hongfeng Mu² , Fei Xu^{1,2}, Wen Zhu², Qing Ye^{1,2},
Yunneng Jizhang², T Kevin Hitchens^{3,4}, Yejie Shi^{1,2} ,
Xiaoming Hu^{1,2} , Rehana K Leak⁵, C Edward Dixon^{1,6},
Michael VL Bennett⁷ and Jun Chen^{1,2}

Abstract

Long-term neurological recovery after severe traumatic brain injury (TBI) is strongly linked to the repair and functional restoration of injured white matter. Emerging evidence suggests that the anti-inflammatory cytokine interleukin-4 (IL-4) plays an important role in promoting white matter integrity after cerebral ischemic injury. Here, we report that delayed intranasal delivery of nanoparticle-packed IL-4 boosted sensorimotor neurological recovery in a murine model of controlled cortical impact, as assessed by a battery of neurobehavioral tests for up to five weeks. Post-injury IL-4 treatment failed to reduce macroscopic brain lesions after TBI, but preserved the structural and functional integrity of white matter, at least in part through oligodendrogenesis. IL-4 directly facilitated the differentiation of oligodendrocyte progenitor cells (OPCs) into mature myelin-producing oligodendrocytes in primary cultures, an effect that was attenuated by selective PPAR γ inhibition. IL-4 treatment after TBI in vivo also failed to stimulate oligodendrogenesis or improve white matter integrity in OPC-specific PPAR γ conditional knockout (cKO) mice. Accordingly, IL-4-afforded improvements in sensorimotor neurological recovery after TBI were markedly impaired in the PPAR γ cKO mice compared to wildtype controls. These results support IL-4 as a potential novel neurorestorative therapy to improve white matter functionality and mitigate the long-term neurological consequences of TBI.

Keywords

Traumatic brain injury, white matter injury/integrity, OPC differentiation, oligodendrogenesis, PPAR γ

Received 1 May 2020; Revised 5 June 2020; Accepted 12 June 2020

Introduction

Traumatic brain injury (TBI), a leading cause of death and disability in youth and adults, may cause neuronal damage in grey matter and axonal injury in white matter tracts.^{1,2} However, preclinical studies of interventions against TBI largely emphasize neuronal survival in grey matter—rather than protection of white

⁴Department of Neurobiology, School of Medicine, University of Pittsburgh, Pittsburgh, PA, USA

⁵Graduate School of Pharmaceutical Sciences, School of Pharmacy, Duquesne University, Pittsburgh, PA, USA

⁶Department of Neurosurgery, University of Pittsburgh, Pittsburgh, PA, USA

⁷Dominick P. Purpura Department of Neuroscience, Albert Einstein College of Medicine, Bronx, NY, USA

*These authors contributed equally to the work.

¹Geriatric Research, Education and Clinical Center, Veterans Affairs Pittsburgh Health Care System, Pittsburgh, PA, USA

²Pittsburgh Institute of Brain Disorders & Recovery and Department of Neurology, University of Pittsburgh, Pittsburgh, PA, USA

³Animal Imaging Center, School of Medicine, University of Pittsburgh, Pittsburgh, PA, USA

Corresponding author:

Jun Chen, Department of Neurology, University of Pittsburgh, 3500 Terrace Street, S-507 BST, Pittsburgh, PA 15213, USA.
Email: chenj2@upmc.edu

matter—and most of these interventions have failed to translate when tested in clinical trials.³ Indeed, accumulating studies show that the extent of white matter disruption is a more sensitive predictor of neurological outcomes after TBI.^{4,5} Therefore, finding therapies that can support white matter integrity after TBI is an urgent, unmet need.

White matter injury induced by TBI is characterized by loss of the myelin sheath (demyelination) and axonal degeneration.^{6,7} The injured brain only shows limited white matter repair, with insufficient axonal regeneration and remyelination. After brain injury, oligodendrocyte precursor cells (OPCs) actively proliferate, but most of the newly generated OPCs fail to differentiate into mature myelin-producing oligodendrocytes (OLs), resulting in inadequate remyelination.^{8,9} Thus, interventions that induce OPC differentiation and oligodendrogenesis may promote white matter recovery after TBI.

Interleukin-4 (IL-4) is an anti-inflammatory cytokine secreted from a variety of immune cells and serves critical roles in the brain under physiological and pathological conditions.¹⁰ After brain injury, IL-4 receptors are widely expressed in brain cells, including microglia, astrocytes, and oligodendrocytes. Acting through these receptors, IL-4 participates in a wide variety of processes, such as regulation of inflammation, cell differentiation, and trophic factor production.^{11,12} Our previous studies revealed that IL-4 regulates microglia/macrophage polarization towards anti-inflammatory phenotypes and is critical for functional recovery after brain ischemia.^{11,13} Through its anti-inflammatory properties, IL-4 has also been reported to promote white matter integrity after cerebral hypoperfusion.¹⁴ In addition to its classic role in immune modulation, our recent study found that IL-4 promotes OPC differentiation and axonal remyelination after cerebral ischemia through the PPAR γ signaling axis.¹⁵ However, whether IL-4 will facilitate oligodendrogenesis and white matter recovery in TBI is still unknown.

The current study is the first to investigate IL-4 treatment in a murine animal model of TBI. We report the post-TBI intranasal administration of IL-4 as a novel intervention against white matter injury. IL-4 treatment improved OPC differentiation, oligodendrogenesis, white matter integrity, and long-term sensorimotor function recovery after TBI. In addition, we discovered that the white matter protection and functional recovery afforded by IL-4 are mediated by activation of PPAR γ signaling within oligodendrocytes. Overall, these findings indicate that activation of the IL-4/PPAR γ signaling cascade may be a viable clinically relevant therapeutic option to improve long-term sensorimotor outcomes after TBI.

Materials and methods

Animals

All experimental procedures were in accordance with the National Institutes of Health *Guide for the Care and Use of Laboratory Animal* and the ARRIVE guidelines (*Animal Research: Reporting in Vivo Experiments*)¹⁶ and approved by the University of Pittsburgh Institutional Animal Care and Use Committee. All animals were housed in a temperature- and humidity-controlled facility with a 12-h light/dark cycle. Food and water were available ad libitum. We made all efforts to reduce animal suffering and the number of animals used.

Male wildtype (WT) and PPAR γ conditional knockout (cKO) mice were used at 10–12 weeks of age. PPAR γ cKO mice (PDGFR α ^{CreER(+/-)} PPAR γ ^{flox/flox}) were generated by crossing PPAR γ ^{flox/flox} mice with PDGFR α ^{CreER} mice, in which Cre recombination is controlled by 4-hydroxytamoxifen and limited to OPCs. WT mice, PPAR γ ^{flox/flox} mice, and PDGFR α ^{CreER} mice were purchased from the Jackson Laboratory (Bar Harbor, ME). As characterized previously for the PDGFR α ^{CreER} mice,¹⁷ 4-hydroxytamoxifen injections resulted in Cre recombination in over 93% of total OPCs in the cortex. PPAR γ cKO mice were obtained by crossing for at least two generations. Conditional knockout of PPAR γ was induced by 4-hydroxytamoxifen injections in 10-week-old PDGFR α ^{CreER(+/-)} PPAR γ ^{flox/flox} mice (75 mg/kg, i.p., once a day for five consecutive days). The total number of animals used is listed in Supplementary Table 1. Mortality rates showed no difference between WT and PPAR γ cKO mice.

Murine model of traumatic brain injury

Fourteen days after the final tamoxifen injection, TBI was elicited by unilateral controlled cortical impact (CCI), as previously described.¹⁸ Briefly, animals were randomly assigned to sham and TBI groups. All animals were anesthetized with 1.5% isoflurane in a 68.5% N₂O/30% O₂ mixture through a nose cone. Under anesthesia, mouse heads were stabilized in a stereotaxic frame and a skin incision was made under aseptic conditions to expose the skull and identify Bregma. A right parietal craniotomy (diameter of 3.5 mm; centered 0.5 mm anterior and 2.0 mm lateral to Bregma) was prepared with a drill to expose the dura and cerebral cortex. CCI was performed with a pneumatically driven CCI device (Precision Systems and Instrumentation, Fairfax Station, VA, USA) utilizing a 3 mm (diameter) flat-tipped impactor to compress the exposed brain dura mater to a depth of 1.5 mm, for a dwell time of 150 ms and at a peak velocity of 3.75 m/s.

Rectal temperatures were kept at $37 \pm 0.5^\circ\text{C}$ constantly during surgery using a heating pad. After surgery, the skin incision was sealed, and mice were placed in a clean cage. Animals in the sham group were subjected to anesthesia and skin incisions, but were not subjected to craniotomy preparation or CCI.

Preparation and intranasal administration of IL-4 liposome nanoparticles

IL-4 liposome nanoparticles were prepared as described.¹⁵ Briefly, lecithin (150 mg) and cholesterol (15 mg) were dissolved in a chloroform-methanol mixed solution (3:1, volume:volume; total volume: 5 mL), and then evaporated under vacuum distillation to form a lipid layer. Recombinant endotoxin-free IL-4 protein (1 mg, Peprotech, Rocky Hill, NJ, USA) dissolved in water (5 mL) was added to the lipid layer for hydration for 30 min. Ultrasonic probes were then applied to homogenize the mixture for 15 min in an ice bath. After this, the mixture was filtered through a 0.45- μm membrane and followed by ultra-filtered with centrifugal filter units (100-KDa cutoff) to remove the free IL-4 protein. Dynamic light scattering (DLS) was used to evaluate the particle size, polydispersity index, and zeta potential of IL-4 protein-loaded liposomes.¹⁵ The concentration of IL-4 protein in the liposomes was examined by the bicinchoninic protein determination kit (Thermo Fisher Scientific, Pittsburgh, PA, USA).

Animals were randomly distributed to receive intranasal administration of vehicle or IL-4 (50 $\mu\text{g}/\text{kg}$ body weight) nanoparticle, starting at 6 h and repeated on days 1–7 (daily), and then on days 14, 21, and 28 after TBI. One-time intranasal administration of this dose resulted in significant elevation of IL-4 concentration in various brain regions, including cortex (CTX), striatum (STR), corpus callosum (CC) and external capsule (EC), for up to 12–24 h, and the above administration regimen showed efficacy in the mouse model of focal cerebral ischemia and reperfusion.¹⁵ Briefly, nanoparticle-packed IL-4 was diluted to the final concentration of 0.1 $\mu\text{g}/\mu\text{L}$. Under isoflurane anesthesia, five drops ($\sim 2 \mu\text{L}/\text{drop}$) of vehicle or diluted IL-4 nanoparticles were delivered alternately into each nostril, with a 2-min interval between drops.

Behavior tests

Foot fault test. The foot fault test was performed as described previously,¹⁹ to assess sensorimotor coordination during spontaneous locomotion. Briefly, an elevated grid surface (40 cm (L) \times 20 cm (W) \times 30 cm (H)) with a grid opening of 2.25 cm^2 (1.5 cm \times 1.5 cm square) was prepared. Mice were placed on the grid

surface and videotaped from below the grid for 1 min. The videotapes were analyzed by a blinded investigator for the number of total steps and the number of foot faults made by the left limbs (impaired side; contralateral to brain lesion). The number of total steps reflects gross locomotor function. Foot faults were determined when the mouse misplaced its left forepaw or hind paw, such that the paw fell through the grid opening, and these numbers were presented as a percentage of total steps.

Cylinder test. This test was employed to assess forelimb asymmetry before and after TBI.²⁰ Mice were placed in a transparent cylinder (9 cm in diameter; 15 cm in height) and videotaped from above for 8–10 min. In exploring the cylinder, mice typically exhibit spontaneous rears contacting the cylinder wall with the right forelimb (R), the left forelimb (L), or both forelimbs (B). Behavior was recorded and analyzed by an investigator blinded to treatment groups. As the brain injury was in the right hemisphere, the preference for the impaired left forelimb (the contralateral forepaw) was calculated by the following formula: $(L + B/2)/(L + R + B) \times 100\%$. Mice that exhibited fewer than 10 rears or a baseline preference for either forelimb before TBI were excluded from further analyses.

Rotarod test. The Rotarod test was selected to test motor coordination and dysfunction, as described before.²¹ Mice were put on an rotating rod, the speed of which accelerated from 4 to 40 r/min within 5 min. Mice were trained for three days (three trials daily) before surgery and then tested three times per day at the indicated testing day after TBI. Mice were allowed to have 5 min of intermission between trials each day. The total time spent on the accelerating rod was fixed and recorded digitally by the Rotarod machine when the mice fell off the rod. The averages of three trials on the last day of training were counted as the baseline value. After surgery, the averages of three trials were recorded on the days indicated in the figures.

Measurement of tissue loss

Animals were euthanized and followed by perfused with saline and 4% paraformaldehyde (Sigma-Aldrich; St. Louis, MO) in PBS. Brains were harvested and then submerged in 30% sucrose in PBS two days for cryoprotection. Coronal brain sections (25 μm) were prepared using a freezing microtome (model CM3050S; Leica Biosystems, Wetzlar, Germany). Five or six equally spaced coronal brain sections were stained with mouse anti-Microtubule-Associated Protein 2 antibodies (MAP2; Millipore, 1:500 Burlington, MA) or Rabbit anti-NeuN (Millipore, 1:500, St. Louis, MO), as

described in the following section. Brain tissue loss was calculated by ImageJ software. The total volume of tissue loss was analyzed by subtracting the non-injured volume of the ipsilateral hemisphere from the entire volume of the contralateral hemisphere.

Immunofluorescence and image analysis

Coronal sections were collected as described above and subjected to immunofluorescent staining. Free-floating brain sections were incubated in 1% PBST (PBS with 1% Triton) for 15 min after a series of washes, and then blocked with 5% donkey serum for 1 h. After another series of washes, brain sections were incubated in primary antibodies at room temperature for 1 h and then overnight at 4°C. After PBS washes, brain sections were incubated on the following day with donkey secondary antibodies conjugated to AlexaFluor 488 or Cy3 (1:1000, Jackson ImmunoResearch Laboratories, West Grove, PA, USA), for 1 h at room temperature. After a series of washes, brain sections were mounted and coverslipped with Fluoromount-G containing 4', 6-diamidino-2-phenylindole (DAPI; Southern Biotech, Birmingham, AL), to stain cell nuclei. The following primary antibodies were used: rabbit anti-myelin basic protein (MBP; Abcam, 1:500; Cambridge, MA), mouse anti-nonphosphorylated neurofilaments (SMI32; Calbiochem, 1:1000; San Diego, CA), rabbit anti-Neurofilament heavy chain subunit 200 (NF200; Abcam, 1:500; Cambridge, MA), rabbit anti-beta-amyloid precursor protein (β -APP; ThermoFisher Scientific, 1:500), rabbit anti-NG2 (Millipore, 1:400; Temecula, CA), mouse anti-APC (Millipore, 1:400; Burlington, ME). Fluorescence images were taken by either an Olympus Fluoview FV1000 confocal microscope and FV10-ASW 2.0 software (Olympus America) or an inverted Nikon Diaphot-300 fluorescence microscope and a SPOT RT slider camera and Meta Series Software 5.0 (Molecular Devices).

Two to three brain sections were selected in each mouse. Two regions of interest (ROIs) in the perilesional cortex and striatum, one ROI in the CC and one ROI in the EC in each brain section were randomly selected and captured using the same imaging parameters. The fluorescence intensity of SMI32, MBP, and NF200, and the number of β -APP particles were calculated in Image J software by an investigator blinded to experimental groups. The ratio of SMI32 to MBP fluorescence intensity was calculated to evaluate white matter injury.

Western blot

After mice were euthanized, fresh brain tissues from the CC and EC areas in the whole brain were quickly extracted and frozen on dry ice. Western blot experiments were performed on the protein extracts.

Standard SDS-polyacrylamide gel electrophoresis was used. Briefly, polyvinylidene difluoride (PVDF) membranes were blocked with 5% nonfat milk for 1 h at room temperature and then followed by incubated with primary antibodies at 4°C overnight. After washing, secondary antibodies were applied to incubate the PVDF membranes for 1 h at room temperature (1:10,000, LI-COR Biosciences, Lincoln, NE). After further washes, the PVDF membranes were scanned and images were taken with the LI-COR Odyssey Infrared Imaging System 9201-550 U (LI-COR Biotechnology, Lincoln, NE). The following primary antibodies were used: rabbit anti-MBP (Abcam; 1:1000, Cambridge, MA), rabbit anti-neurofilament 200 (NF200; Abcam; 1:1000), and mouse anti- β -actin (Sigma-Aldrich, 1:20,000; St. Louis, MO). Images were analyzed by Image J software.

DTI

Diffusion tensor imaging (DTI) was applied to examine white matter integrity at 35 days after TBI.²² Mice were deeply anesthetized with isoflurane and followed by transcardially perfused with 0.9% NaCl and 4% PFA in PBS. Ex vivo brains were harvested with the skull intact to avoid anatomical deformation, and then immersed in 4% PFA overnight at 4°C, followed by storage in PBS. MRI was performed using a Bruker AV3HD 11.7 Tesla/89 mm vertical-bore microimaging system equipped with a Micro2.5 gradient set capable of 1500 mT/m, ParaVision 6.0.1, and a 20 mm quadrature RF resonator (Bruker Biospin, Billerica, MA). After positioning and pilot scans, the entire brain was scanned and the data were collected into a DTI dataset using a multislice spin-echo sequence with 5 A0 images and 30 non-colinear diffusion images. The following parameters were used: TE/TR 22/2800 ms, 2 Averages, 160 × 160 matrices, 16 × 15 mm field of view, 25 slices, 0.5 mm slice thickness, b-value = 3000 s/mm², and $\Delta/\delta = 11.0/5.0$ ms. DSI Studio software (<http://dsi-studio.labsolver.org/>) was used to analyze DTI data. A single ROI encompassing the EC in the ipsilesional or contralesional hemispheres was manually drawn in a blinded manner to determine fractional anisotropy (FA, reflects overall microstructural integrity), mean diffusivity (MD, an inverse measure of the membrane density; generally sensitive to cellularity, edema, and necrosis), and radial diffusivity (RD; λ_+ ; generally sensitive to myelin integrity).²⁷ DSI Studio software was used to generate directionally encoded color (DEC), FA, MD and RD maps.

CAP measurements

Compound action potentials (CAPs) in the CC and EC areas were measured as described previously.²² Briefly,

mice were euthanized and decapitated followed by rapid brain harvest. Coronal brain slices (350 μm) were cut -1.06 mm posterior from Bregma on a Vibratome (Leica) and placed in pre-gassed (95% O_2 /5% CO_2) artificial cerebrospinal fluid (aCSF; NaCl 130 mmol/L, KCl 3.5 mmol/L, NaHCO_3 24 mmol/L, Na_2HPO_4 1.25 mmol/L, CaCl_2 2 mmol/L, MgSO_4 1.5 mmol/L, glucose 10 mmol/L; pH 7.4) for 1 h at 22°C . Brain sections were then removed into a recording chamber where they were constantly perfused and submerged with aCSF (3–4 mL/min) at 22°C . A concentric bipolar stimulating electrode was placed into the CC, approximately 0.9 mm lateral to the midline. A glass extracellular recording pipette (filled with aCSF, 5 to 8 M Ω tip resistance) was placed into the EC, 0.75 mm lateral to the stimulating electrode. The recordings made 0.75 mm from the stimulating electrode were analyzed. Both electrodes were placed at a depth of 50–100 μm on the brain slices, and the signal was adjusted and optimized by an investigator blinded to experimental groups. The input stimuli ranged from 0 to 1750 μA (100 μs duration, delivered at 0.05 Hz). The evoked CAPs were recorded by an Axoclamp 700B (Molecular Devices) and analyzed with pCLAMP 10 software (Molecular Devices). The average waveforms of four successive sweeps in two slices per mouse were quantified. The recording shows two negative peaks, conventionally referred to as N1 and N2, and described further below.

Primary OPC cultures

Primary oligodendrocyte progenitor cell (OPC) cultures were isolated as previously described.²³ Briefly, brains of Sprague Dawley rat pups (postnatal days 1–2, mixed sex) were quickly harvested on ice. After removal of the meninges and blood vessels, brains were triturated and followed by dissociated with Trypsin (0.01%) for 15 min at 37°C . Cells were then washed with ice-cold DMEM and followed by passed through a 70- μm filter. After this, cells were plated onto T-flasks coated with poly-D-lysine and filled with culture media (DMEM/F12 containing 10% heat-inactivated fetal bovine serum, 1 mM sodium pyruvate, 2 mM L-glutamine, 50 U/mL penicillin, 100 μM nonessential amino acids and 50 $\mu\text{g}/\text{mL}$ streptomycin). Cells in the T-flasks were cultured in a humidified incubator at 37°C with 5% CO_2 to grow to confluence (12–14 d in vitro (DIVs)). To remove microglia, the glia-containing flasks were shaken for 1 h at 180 r/min. After this, OPCs were further separated from the astrocyte layer by shaking the flasks at 200 r/min overnight. OPCs were cultured for three to five days in a basal defined medium (BDM: DMEM, 0.1% bovine serum albumin, 50 $\mu\text{g}/\text{mL}$ insulin, 50 $\mu\text{g}/\text{mL}$ human apo-transferrin,

30 nM sodium selenite, 10 nM hydrocortisone, 10 nM D-biotin) with serum-free but containing 10 ng/mL platelet-derived Growth factor AA (PDGF-AA) and 10 ng/mL bFGF. OPCs were stimulated with T3 (50 ng/mL) and CNTF (10 ng/mL) as positive controls to induce oligodendrocyte (OL). Media were exchanged every two days. To examine the role of IL-4 in OPC differentiation, primary OPCs were treated with IL-4 at escalating concentrations (2.5, 5, 10, 20 ng/mL). To mimic TBI in vitro, chondroitin sulfate proteoglycan (CSPG, 50 $\mu\text{g}/\text{mL}$) was added into the medium, and 20 ng/mL IL-4 was applied to treat the CSPG-injured OPCs. OPCs were also treated with the PPAR γ inhibitor GW9662 (0.5 μM) or vehicle (DMSO) for 30 min, followed by co-incubation with IL-4 (0, 10 or 20 ng/mL), T3+CNTF or vehicle for five days. Double immunostaining of mature OL marker MBP and OPC marker NG2 was performed at five days after treatment.

Examination of newly proliferated cells

Cells that had proliferated recently were labeled with the S-phase marker 5-bromo-2'-deoxyuridine (BrdU; Sigma-Aldrich, St. Louis, Missouri), as described previously.²⁴ In brief, BrdU (50 mg/kg of body weight) was injected (i.p.) twice a day, three to six days after TBI. At 35 days after TBI, mice were sacrificed to harvest brains, and coronal brain sections were prepared as described above. Sections were incubated with 1N HCl for 1 h, and then with 0.1 M boric acid (pH 8.5) for 15 min at room temperature. Sections were further blocked with M.O.M. kit (Vector, Burlingame, CA, USA) for 1 h at room temperature to reduce non-specific staining, and followed by incubated with mouse anti-BrdU antibodies (1:1000; BD Biosciences) for 1 h at room temperature, and then overnight at 4°C . After washing on the next day, brain slices were incubated with 488-AffiniPure donkey anti-mouse IgG (1:1000; Jackson ImmunoResearch Laboratories) for 1 h at room temperature.

Oligodendrogenesis was assessed by double-labelling brain sections for BrdU and the OL marker APC. At least two microscopic fields in the CTX and STR, one field in the CC and one field in the EC were sampled in each section. Two to three sections were selected in each mouse. BrdU and APC double immunopositive cells were counted using Image J. Oligodendrogenesis was evaluated as the number of BrdU⁺/APC⁺ cells in the designated fields, divided by the area of the fields in mm^2 .

Statistical analysis

Results are presented as mean \pm standard deviation (SD) or as quartiles for box plots. SPSS software was used for statistical analyses. For each data set, the

Kolmogorov–Smirnov normality test was first performed to determine the data distribution patterns. For normally distributed data (parametric), the Student's *t* test was used for single comparisons or one-way ANOVA and Bonferroni/Dunn post hoc tests for multiple comparisons. For abnormally distributed data (nonparametric), Mann–Whitney U test or Kruskal–Wallis test with Bonferroni/Dunn post hoc tests was used for single and multiple comparisons, respectively. Differences in means across groups with repeated measurements over time were analyzed by the repeated-measures ANOVA and Bonferroni/Dunn post hoc tests. Pearson product linear regression analyses were used to correlate behavior measurements and multiple histological parameters. A *p* value of <0.05 was considered statistically significant. Further details on each comparison can be found in the statistics report (Table S2).

Results

Intranasal administration of IL-4 facilitates long-term sensorimotor recovery after traumatic brain injury

Long-term neurological functions are key parameters to evaluate TBI outcomes.²⁵ To assess the therapeutic efficacy of IL-4 intranasal administration on TBI, the foot fault and cylinder tests were applied to examine sensorimotor functions, before and up to 35 days after TBI (Figure 1(a)). Mice in sham groups showed no difference after they received either vehicle or IL-4 treatment. Therefore, the two groups of sham controls (WT-sham or cKO-sham, treated with vehicle or IL-4) were combined for statistical analysis for all in vivo experiments throughout the study. As expected, TBI induced dramatic sensorimotor deficits, as demonstrated by significant increases in foot fault rates in both forepaws and hind paws (Figure 1(b) and (c)). However, IL-4 treatments attenuated foot fault rates, starting as early as seven days after TBI in the forepaw and five days after TBI in the hind paw (Figure 1(b) and (c)). Forelimb asymmetry was also induced by TBI, as shown by lower contralateral forepaw use in the cylinder test. IL-4 treatment successfully alleviated the asymmetry from 21 days after TBI until the end of the testing period (Figure 1(d)). During the testing period, the total forepaw or hind paw steps in the foot fault test and the total contacts with the cylinder during rearing behavior in the cylinder test showed no differences among groups, suggesting that the impacts of IL-4 and TBI did not arise from clear variations in gross motor abilities (Figure S1(a) to (c)).

To determine whether IL-4-induced recovery of neurological function was associated with preservation of brain tissue, we measured the volume of brain

tissue loss using neuronal MAP2 immunostaining (Figure 1(e)) at 35 days after TBI. The results showed that IL-4 did not prevent gross brain tissue loss, as indicated by the comparable volumes of tissue loss (Figure 1(f)) and cross-sectional areas of tissue loss per section in vehicle versus IL-4-treated mice (Figure S1(d)).

IL-4 promotes the structural integrity of myelin and axonal fibers after traumatic brain injury

Next, we examined potential mechanisms underlying the neurological improvements induced by IL-4 intranasal administration post-injury. Accumulating evidence demonstrates that white matter integrity is essential for maintaining neurological function after TBI.^{22,26} Thus, we investigated white matter histological indicators. First, we assessed the microstructure of white matter components by double-staining brain sections for MBP (marker for myelin) and SMI32 (marker for demyelinated axons) at 35 days after TBI (Figure 2(a) and (b)). TBI induced the expected disruption in myelin sheaths, as identified by a decrease of MBP and a concurrent increase in SMI32 intensity (Figure 2(a)). A significant increase in the SMI32/MBP ratio was observed in the peri-lesional CC and STR areas after TBI (Figure 2(c) to (f)). However, IL-4 treatment successfully attenuated myelin disruption in the CC (Figure 2(c)). To investigate whether the improvement in myelin integrity was associated with sensorimotor recovery, Pearson product linear regression analyses were performed on SMI32/MBP ratios and sensorimotor functions at 35 days after TBI. The foot fault rate of the forepaw positively and moderately correlated with SMI32/MBP ratios in the CC, CTX, and STR (Figure S2(a) to (d)). In addition, contralateral forepaw use correlated negatively with SMI32/MBP ratios in the CC, CTX, and STR (Figure S2(e) to (h)). These data suggest that improved myelin integrity may be an important factor in IL-4-induced neurological protection.

To better characterize the integrity of the myelin sheath and axon, we then measured expression of the myelin marker MBP and axonal neurofilament marker NF200 in the CC and EC areas by semiquantitative immunoblotting 35 days after TBI (Figure 2(g)). TBI induced loss of both MBP and NF200 in the CC and EC areas, while IL-4 treatments completely abolished these changes (Figure 2(h) and (i)). These collective findings strongly support the hypothesis that post-TBI treatment with IL-4 promotes axon and myelin integrity.

Aside from oligodendroglial myelin sheaths, we also immunostained neuronal axons with NF200 at 35 days after TBI (Figure 2(j) to (k)). TBI induced considerable axon damage in both CC and STR areas, as identified

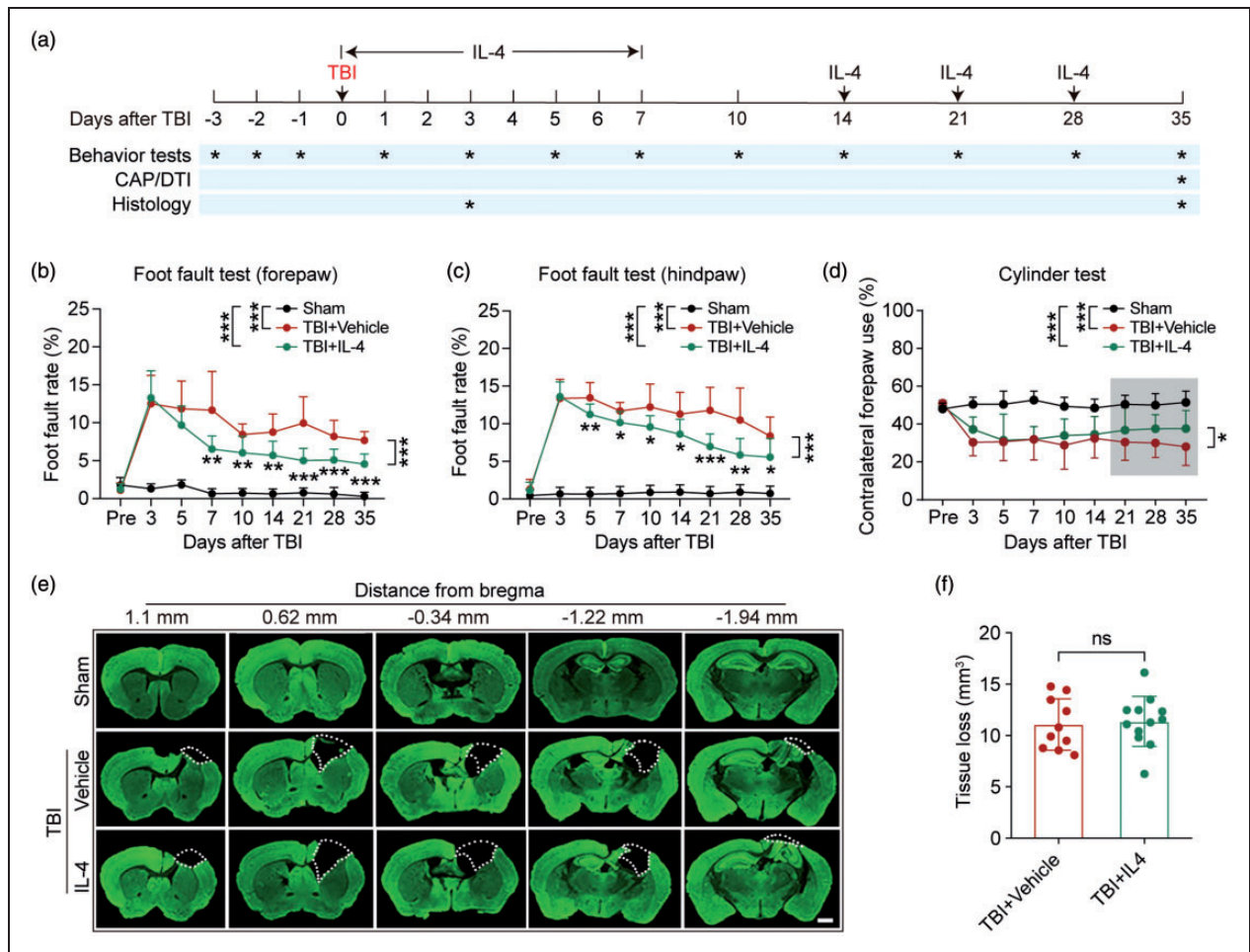


Figure 1. Delayed intranasal IL-4 delivery promotes long-term sensorimotor recovery after TBI. Mice received intranasal administrations of IL-4 (50 μ g/kg) or vehicle starting at 6 h after CCI and repeated on days 1–7 (daily) and then on days 14, 21, and 28 after CCI. Long-term sensorimotor function and brain tissue loss were analyzed. (a) Illustration of experimental timeline. (b–c) Foot fault test. The foot fault rates of the left forelimb (b) and hindlimb (c) were quantified. (d) Cylinder test. Contralateral forepaw use was calculated. The shadowed region indicates the portion of data that displayed significant differences (21–35 days). (e) Five coronal sections spanning from 1.10 mm anterior to Bregma to 1.94 mm posterior to Bregma were stained for the neuronal somatodendritic marker MAP2 at 35 days after TBI. The dashed line defines the border of tissue loss. Scale bar = 1 mm. (f) Blinded quantification of volume of tissue loss, defined as the viable tissue volume of the ipsilateral hemisphere subtracted from the viable tissue volume of the contralateral hemisphere. * $p < 0.05$, ** $p < 0.01$, *** $p < 0.001$, ns: no significance. A two-way repeated measures ANOVA with Bonferroni post hoc was used in b–d. Unpaired t test was used in f. Foot fault test: $n = 8$ in sham group, $n = 12$ in TBI+Vehicle and TBI+IL-4 group. Cylinder test: $n = 10$ per group in cylinder test. Tissue loss: $n = 10$ in TBI+Vehicle group, $n = 12$ in TBI+IL-4 group.

by loss of NF200 intensity, whereas IL-4 treatment partially restored axon integrity in the CC and STR (Figure 2(k)). Using Pearson product linear regression analyses, we found that axon integrity in the CC and STR areas correlated strongly with sensorimotor functions 35 days after TBI (Figure S2(i) to (n)). These results suggest that post-TBI treatment with IL-4 preserves axonal integrity, which appears to be more closely related with sensorimotor recovery than myelin integrity *per se*.

Next, we investigated whether IL-4 treatment reduces axonal injury at acute injury stages by labeling brain sections collected three days after TBI with antibodies against NF200 and the axonal damage marker β -APP (Figure 2(l)). The numbers of β -APP⁺ particles located along the NF200⁺ axon neurofilaments in the perilesional CC, EC and STR were calculated. TBI dramatically increased β -APP⁺ particles along the neurofilaments, whereas IL-4 treatments decreased the same measure, in all three regions examined (Figure 2(m)). Taken together, these data demonstrate that intranasal

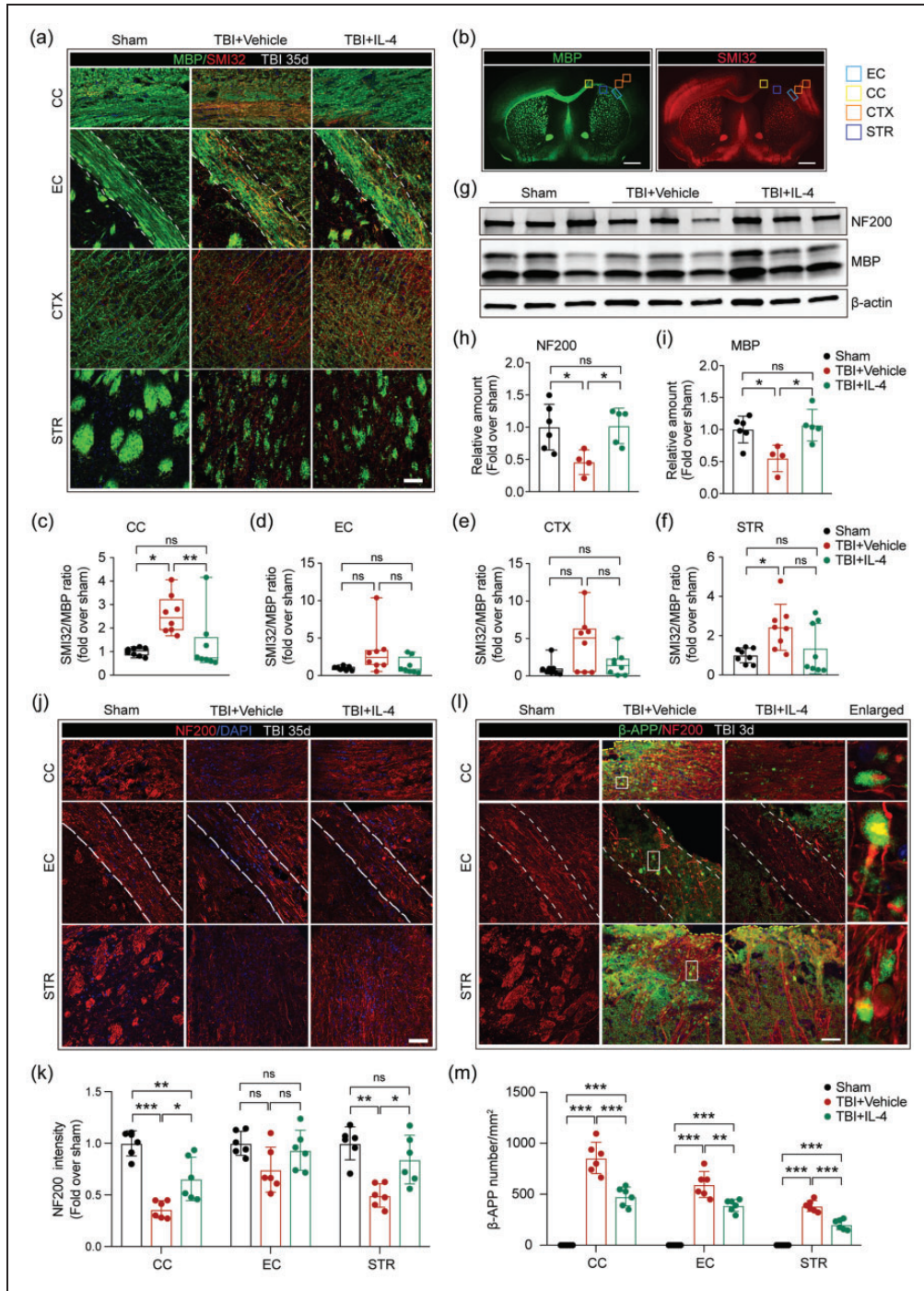


Figure 2. IL-4 treatment restores the structural integrity of white matter after TBI. (a) Representative high-power images of MBP and SMI32 immunostaining in the peri-lesional corpus callosum (CC), external capsule (EC), cortex (CTX), and striatum (STR) at 35 days after TBI. The dotted white lines trace the boundaries of the EC. Scale bar = 50 μ m. (b) Representative low-power images of MBP and SMI32 immunostaining in coronal brain sections. Squares indicate the areas where images were captured in panel A. Scale bar = 1 mm. (c–f) Quantification of the ratio of SMI32/MBP in CC, EC, CTX, and STR. $n = 8$ per group. (g) Representative images of NF200 and MBP bands by Western blot. (h, i) Quantification of NF200 (h) and MBP (i) expression in Western blots. $n = 6$ in sham group, $n = 4$ in TBI+Vehicle group, $n = 5$ in TBI+IL-4 group. (j) Representative high-power images of NF200 staining in the CC, EC, and STR at 35 days after TBI. Scale bar = 50 μ m. The dotted white lines trace the boundaries of the EC. Nuclei were labeled with DAPI (blue). (k) Quantification of the intensity of NF200 immunosignal in the CC, EC, and STR areas. $n = 6$ per group. (l) Representative high-power images of NF200 and β -APP immunostaining in the CC, EC, and STR at three days after TBI. The dotted white lines trace the boundaries of EC. White squares indicate where the enlarged images in column 4 were taken. Scale bar = 50 μ m. (m) Quantification of the number of β -APP immunopositive particles in the peri-lesional CC, EC, and STR areas. $n = 6$ per group. * $p < 0.05$, ** $p < 0.01$, *** $p < 0.001$, ns: no significance, by one-way ANOVA followed by Bonferroni post hoc or Kruskal–Wallis test with Dunn post hoc.

administration of IL-4 protects the structural integrity of axon projections during both acute and chronic stages of TBI.

IL-4 enhances the functional integrity of white matter after traumatic brain injury

Ex vivo diffusion tensor imaging (DTI) scans were performed to evaluate the integrity of white matter in the EC area 35 days after TBI or sham operation (Figures 3(a) and S3(a) and (b)). Increased mean diffusivity (MD) and radial diffusivity (RD) indicate loss of white matter integrity.²⁷ Compared with the sham-operated group, the TBI and vehicle-treated group displayed the expected increases in MD and RD values, while TBI-subjected mice treated with IL-4 showed significant reductions in the same measures, suggesting protection of white matter integrity by IL-4 (Figure 3 (b) and (c)). Pearson product linear regression analyses revealed that MD and RD values correlated positively with forepaw foot-fault rates (Figure 3(d) and (e)), and correlated negatively with the rate of contralateral forepaw use in the cylinder test (Figure S3(e) and (f)). Fractional anisotropy (FA) and axial diffusivity (AD) also indicate white matter integrity.²⁷ The FA value decreased significantly after TBI, revealing disrupted white matter (Figure S3(c)). However, neither parameter was sensitive enough to evaluate IL-4-induced white matter changes in the current experiment (Figure S3(c) and (d)).

We investigated collective axon conduction properties to continue to assess the functional integrity of white matter at 35 days after TBI. Evoked compound action potentials (CAPs) exhibit an early downward peak, representing fast-conducting myelinated axons (N1), and a late downward peak, representing slow-conducting unmyelinated axons (N2) (Figure 3(f) and (g)). The velocity of N1 and N2 transduction showed no difference after TBI or IL-4 treatments (Figure S3(g) and (h)). However, the amplitudes of the N1 and N2 segments were reduced at 35 days after TBI (Figure 3(h) and (i)), revealing impaired conduction through both myelinated and unmyelinated axons. IL-4-treated mice showed less reduction in N1 amplitude after TBI, suggesting superior myelinated axon transduction compared to mice in vehicle-treated group (Figure 3(h)). Furthermore, the amplitude of N1 showed a statistical trend towards a negative correlation with the forepaw foot fault rate (Figure 3(j), $p = 0.052$), but not with the rate of contralateral forepaw use in the cylinder test (Figure S3(i)). As the amplitude of N2 showed no difference between vehicle and IL-4-treated mice, we did not find significant correlations between N2 amplitudes and the behavior measurements (Figures 3(k) and S3(j)).

These data suggest that IL-4 treatment protects the electrophysiological properties of myelinated axons, which is likely to contribute significantly to improvements in sensorimotor function.

IL-4 directly encourages OPC differentiation into mature oligodendrocytes in a PPAR γ -dependent manner

We investigated the impact of IL-4 on OPC differentiation, as mature OLs form the myelin sheaths and are the major component of white matter.²⁸ Previous studies have reported that IL-4 receptors are expressed in OPCs.¹¹ In the present study, IL-4 was added directly to primary OPC cultures at increasing concentrations, from 2.5 to 20 ng/mL. At DIV 5, the number of NG2⁺ OPCs and MBP⁺ mature OLs was analyzed to evaluate OPC differentiation (Figure 4(a) and (b)). IL-4 directly promoted OPC differentiation at all concentrations, especially at 10 and 20 ng/mL, at which its efficacy was comparable to our positive control, the prodifferentiation T3 cocktail (Figure 4(c)). These results are consistent with our recent observations on the effect of IL-4 in promoting OPC differentiation.¹⁵

We have determined the effect of IL-4 in the presence of chondroitin sulfate proteoglycans (CSPG), which tends to accumulate in TBI lesions and forms a non-permissive environment that restricts OPC differentiation and cell survival.²⁹ IL-4 treatment (20 ng/mL) significantly increased MBP⁺ OLs in cultures (Figure 4 (d) and (e)), indicating that IL-4 may be able to promote OPC differentiation into mature OLs under TBI-relevant conditions. PPAR γ is a ligand-dependent transcription factor that belongs to the hormone nuclear receptor superfamily.³⁰ Agonists of PPAR γ are known to promote the differentiation of OPCs into OLs.^{31,32} On this backdrop, we investigated whether IL-4-induced OPC differentiation in primary OPCs is mechanistically dependent on PPAR γ signaling.³³ Indeed, the selective PPAR γ antagonist 2-chloro-5-nitro-N-phenylbenzamide (GW9662)¹⁵ significantly decreased the number of OLs in cultures after treatment with 10 or 20 ng/mL IL-4 (Figure 4(f) and (g)). These data suggest that IL-4 can directly induce OPC differentiation, in a partially PPAR γ -dependent manner.

IL-4 treatment promotes oligodendrogenesis by 35 days after TBI

Next, we investigated if IL-4 treatment also promotes oligodendrogenesis in vivo. Newly generated mature OLs were labeled in brain sections with antibodies against BrdU (marker for newly generated cells) and APC (marker for mature OLs) 35 days after TBI. The density of BrdU⁺APC⁺ cells (newly generated mature

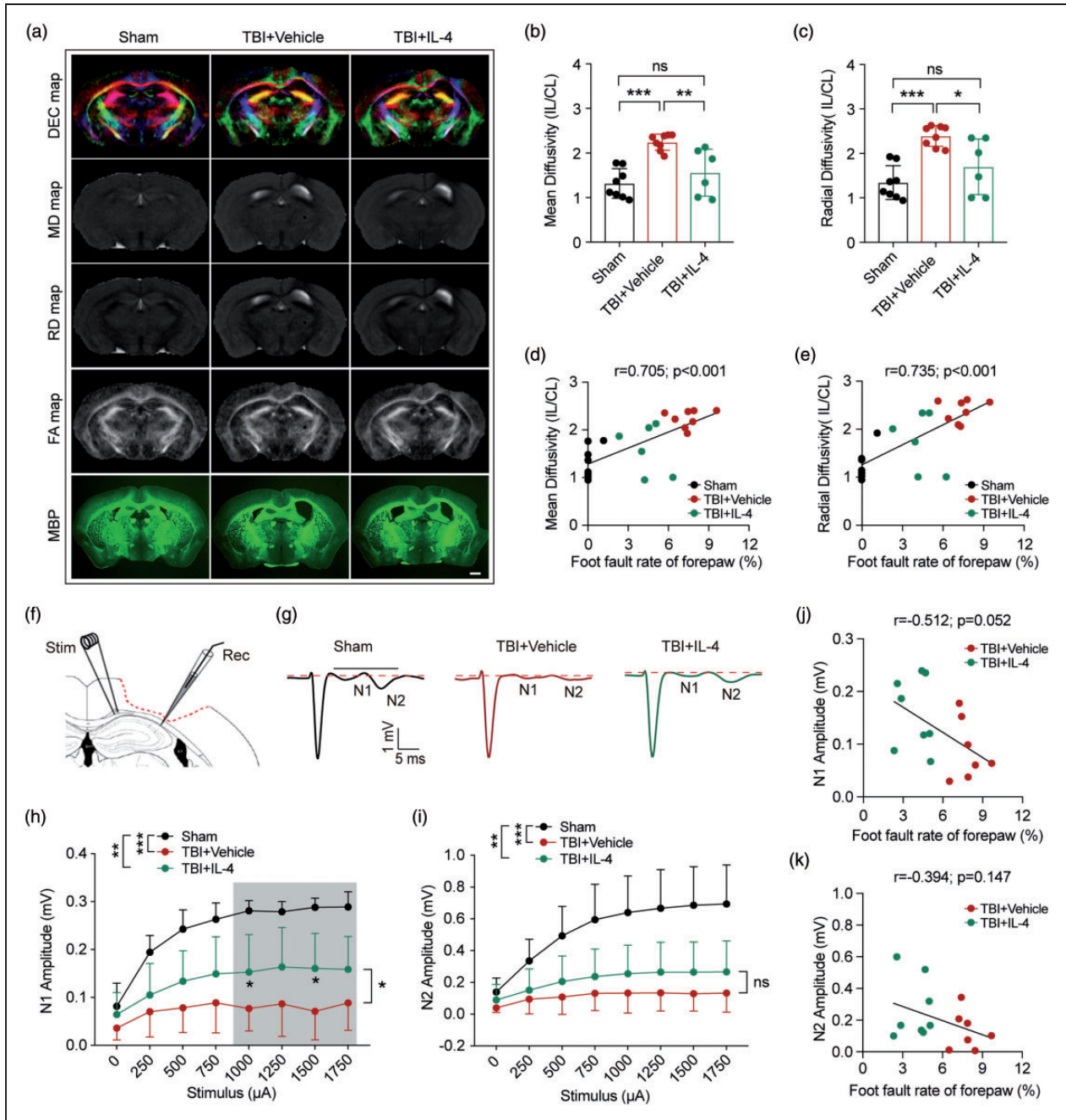


Figure 3. IL-4 improves the physiological function of myelinated fibers after TBI. (a) Representative diffusion encoded color (DEC), mean diffusivity (MD), radial diffusivity (RD), and fractional anisotropy (FA) maps of ex vivo virtual coronal slices and MBP immunostained coronal brain sections at 35 days after TBI. Scale bar = 1 mm. (b, c) Quantification of MD (b) and RD (c) values in the EC. IL: ipsilateral hemisphere, CL: contralateral hemisphere. $n = 8$ in sham and TBI+Vehicle group, $n = 6$ in TBI+IL-4 group. * $p < 0.05$, ** $p < 0.01$, *** $p < 0.001$, ns: no significance, as per one-way ANOVA and Bonferroni post hoc. (d, e) The Pearson correlation between foot fault rate of forepaw (%; foot fault test) and MD (d) or RD values (e). $n = 6-8$ per group. (f-g) Electrophysiological analyses of coronal slices prepared from sham, TBI+Vehicle, and TBI+IL-4 mice at 35 days after TBI. (f) Schematic illustration of the position of the stimulating ("Stim") and recording ("Rec") electrodes in CC/EC. (g) Representative curves of CAPs in myelinated N1 fibers and unmyelinated N2 fibers. (h-i) Quantification of the amplitude of evoked CAPs in N1 and N2 fibers. * $p < 0.05$, *** $p < 0.001$, ns: no significance. Two-way ANOVA followed by Bonferroni post hoc test. $n = 7$ in sham and TBI+Vehicle group, $n = 8$ in TBI+IL-4 group. (j, k) Pearson correlation between foot fault rate of forepaw (%; foot fault test) and N1 amplitude (j) or N2 amplitude (k).

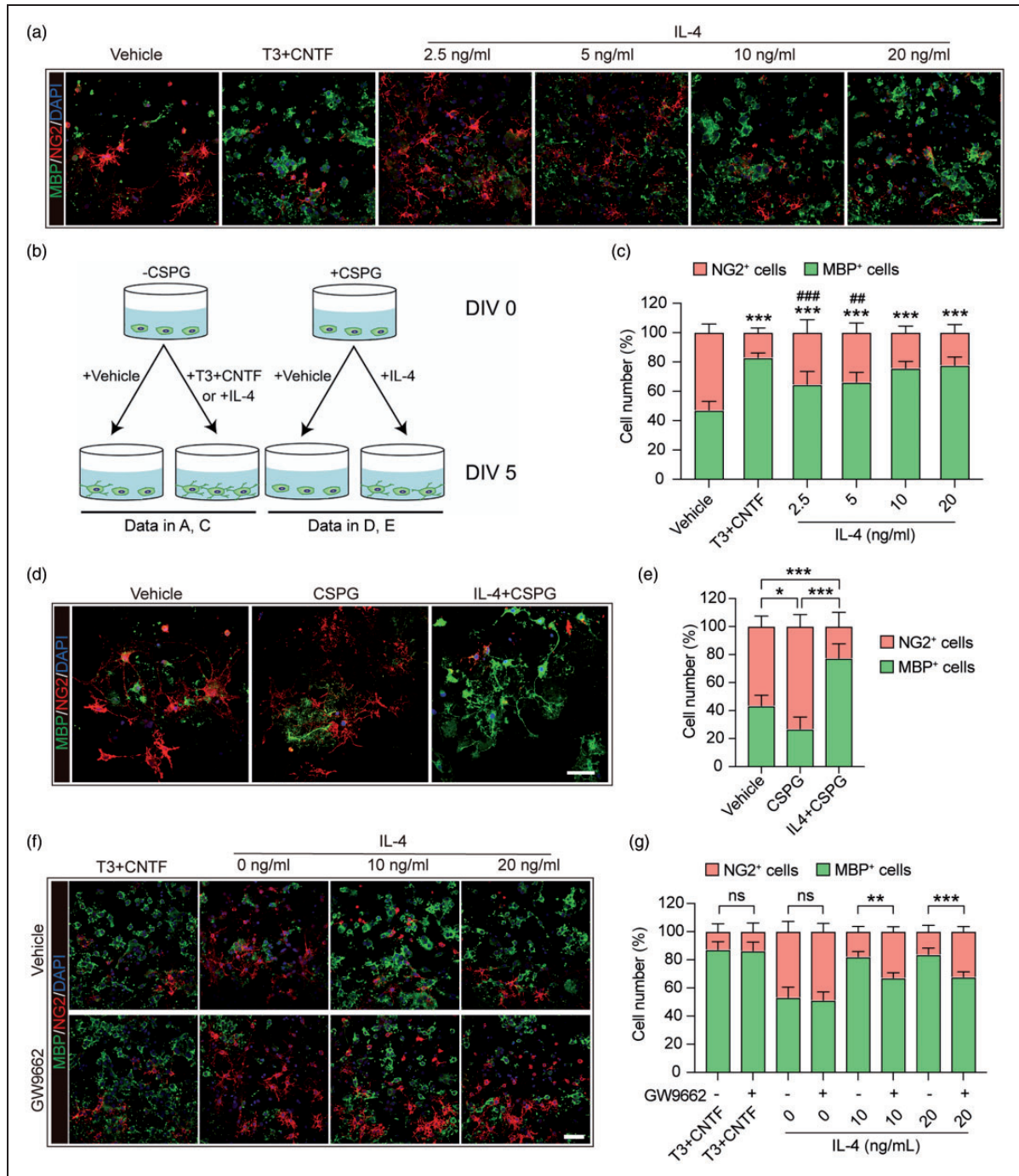


Figure 4. IL-4 directly improves primary OPC differentiation into mature oligodendrocytes in a PPAR γ -dependent manner. (a) Primary OPC cultures were treated with vehicle (PBS), T3 (50 ng/mL) + CNTF (10 ng/mL) or escalating concentrations of IL-4 for five days. Cells were triple-stained with MBP (green), NG2 (red), and DAPI (blue). Scale bar = 50 μ m. (b) Schematic illustration of the experimental design in a, c, d, and e. (c) Quantification of MBP⁺ cells and NG2⁺ cells (as percentages of total cells) in panel A. *** p < 0.001 versus vehicle, #### p < 0.001 versus T3 + CNTF by one-way ANOVA and Bonferroni post hoc. (d) Primary OPC cultures were treated with vehicle (PBS), CSPG (50 μ g/mL), or CSPG + IL-4 (20 ng/mL) for five days, and then immunostained for MBP (green) and NG2 (red). Nuclei were labeled with DAPI (blue). Scale bar = 50 μ m. (e) Quantification of MBP⁺ cells and NG2⁺ cells as percentages of total cells. * p < 0.05, *** p < 0.001 by one-way ANOVA and Bonferroni post hoc. (f) Primary OPC cultures were treated with vehicle (DMSO) or GW9662, a PPAR γ antagonist, followed by T3+CNTF and two concentrations of IL-4 for five days. Cells were then immunostained for MBP (green) and NG2 (red), and nuclei were labeled with DAPI (blue). Scale bar = 50 μ m. (g) Quantification of MBP⁺ cells and NG2⁺ cells as percentages of total cells. ** p < 0.01, *** p < 0.001, ns: no significance by t -test or Mann-Whitney U test. Six fields from three independent experiments were quantified.

OLs) in the perilesional CC, EC, CTX, and STR was measured (Figure 5(a) to (c)). TBI induced spontaneous oligodendrogenesis in all regions examined, and IL-4 treatments significantly promoted the generation of mature oligodendrocytes in the peri-lesional CC and

CTX (Figure 5(d) to (g)). The increase in oligodendrogenesis elicited by IL-4 may underlie the robust improvements in neurological functions. As expected, Pearson product linear regression analysis showed that the number of BrdU⁺APC⁺ cells in the CC displayed a

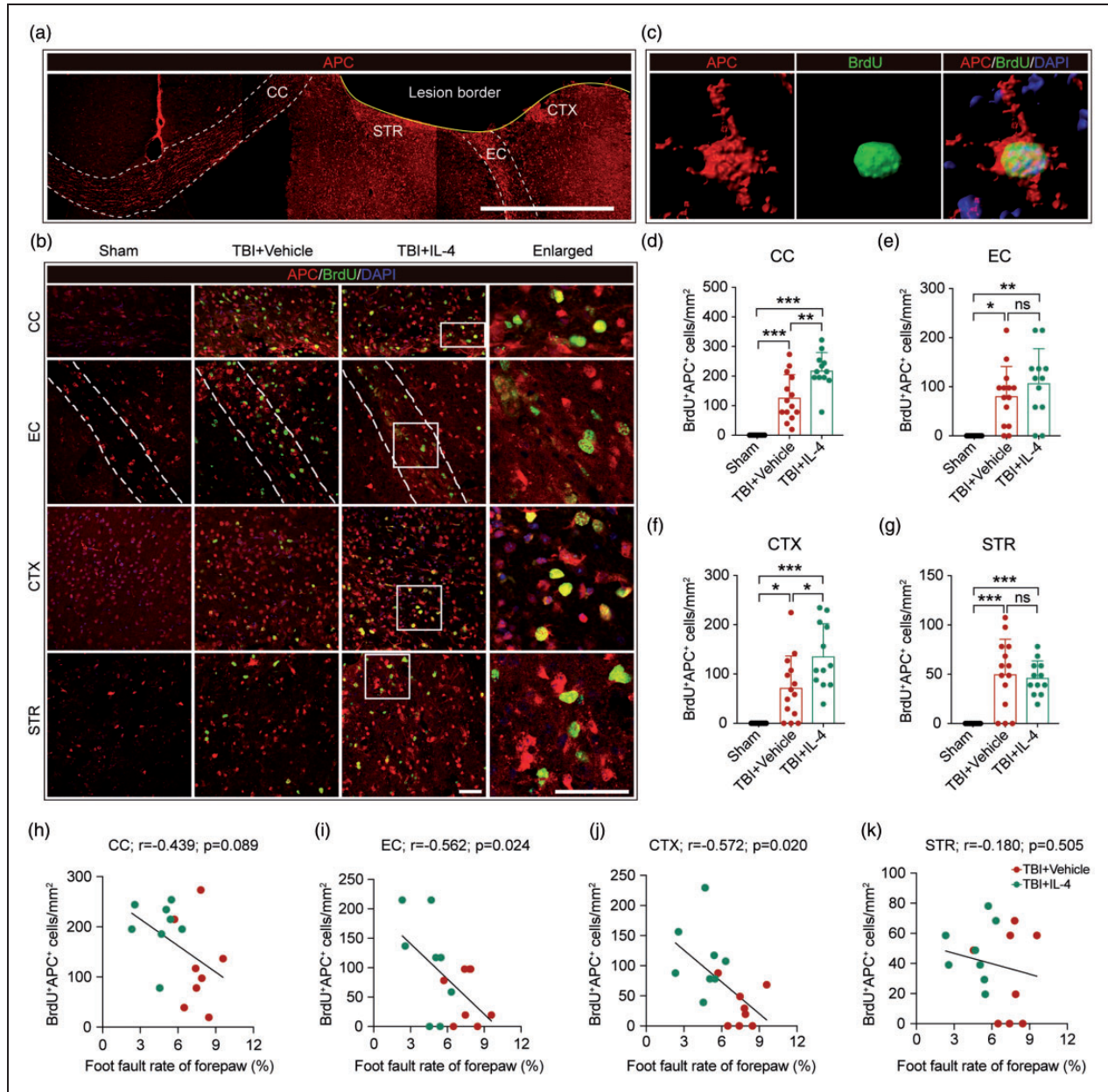


Figure 5. IL-4 treatment promotes oligodendrogenesis in peri-lesional areas after TBI in vivo. (a) Representative low-power images of APC immunostaining in the coronal plane. Scale bar = 500 μ m. (b) Representative high-power images of BrdU and APC double immunostaining in the CC, EC, CTX, and STR at 35 days after TBI. Nuclei were stained with DAPI. Scale bar = 50 μ m. The dotted white lines trace the boundaries of the EC. The white squares in the third column indicate where the enlarged images in the fourth column were captured. (c) Representative images showing a newly generated OL by 3D rendering with Imaris software. (d–g) Quantification of BrdU⁺APC⁺ cells in the CC, EC, CTX, and STR areas. * p < 0.05, ** p < 0.01, *** p < 0.001, ns: no significance, by one-way ANOVA followed by Bonferroni post hoc. n = 8 in sham group, n = 14 in TBI+Vehicle group, n = 12 in TBI+IL-4 group. (h–k) Pearson correlations between the foot fault rate of the forepaw (%; foot fault test) and BrdU⁺APC⁺ cell counts in the CC, EC, CTX, and STR. n = 8 per group.

statistical trend toward a negative correlation with forepaw foot fault rates (Figure 5(h), $p=0.089$). In addition, BrdU⁺APC⁺ cells in the EC and CTX (but not STR) significantly and negatively correlated with the forepaw foot fault rate (Figure 5(i) to (k)). These data demonstrate that IL-4 treatment boosts the levels of oligodendrogenesis within 35 days after TBI in vivo, leading to improvements in neurological functions.

IL-4 treatments fail to enhance oligodendrogenesis after TBI in the absence of oligodendroglial PPAR γ

The data collected thus far suggested that IL-4 improves OPC differentiation into mature OLs in a PPAR γ -dependent manner in vitro. Thus, we proceeded to test whether activation of the PPAR γ signaling axis by IL-4 could promote oligodendrogenesis in the in vivo TBI model, using a transgenic mouse (PPAR γ cKO) strain to specifically knock out PPAR γ within OPCs. Conditional knockout of PPAR γ in OPCs did not impair spontaneous OL regeneration after TBI, as exhibited by considerable numbers of BrdU⁺APC⁺ cells in the CC, EC, CTX, and STR in PPAR γ cKO mice at 35 days after TBI (Figure 6(a) to (e)). However, the capacity of IL-4 to further increase the numbers of newly generated BrdU⁺APC⁺ OLs was abolished when the expression of PPAR γ was absent in OPCs (Figure 6(b) to (e)). These collective results suggest that PPAR γ activation induced by IL-4 is essential for both OPC differentiation in vitro and oligodendrogenesis in vivo.

Conditional knockout of oligodendroglial PPAR γ abolishes IL-4-induced white matter protection and weakens IL-4-afforded neurological protection after TBI

Finally, we investigated the impact of IL-4 treatment on white matter integrity in PPAR γ cKO mice after TBI. TBI led to significant white matter demyelination in the CC, CTX, and STR, as evidenced by increased SMI32/MBP ratios in PPAR γ cKO mice (Figure 7(a) to (e)). Unlike in WT mice, intranasal IL-4 administration failed to protect myelin integrity in all regions examined in PPAR γ cKO mice (Figure 7(b) to (e)). Conditional knockout of PPAR γ in OPCs did not change the protein expression of NF200 and MBP in CC and EC areas in sham-operated mice (Figure S4(a) and (b)). Consistently, IL-4 treatment also failed to increase the protein expression levels of NF200 or MBP after TBI in PPAR γ cKO mice (Figure S4(c) and (d)). The same as WT mice, PPAR γ cKO mice in sham groups showed no difference after they received vehicle or IL-4 treatment. Sham-operated PPAR γ cKO mice showed no impairment in sensorimotor functions,

as evidenced by similar sensorimotor abilities with sham-operated WT mice (Figure S5(a) to (d)). However, PPAR γ cKO minimized IL-4-induced behavioral improvement after TBI, as no statistical difference was observed between vehicle and IL-4-treated PPAR γ cKO mice in the cylinder test (Figure 7(f)). The Rotarod test was also applied as an indicator of motor coordination and balance. However, IL-4 treatment did not exert protective effects in PPAR γ cKO mice after TBI, as suggested by comparable latencies to fall in vehicle versus IL-4-treated mice (Figure 7(g)). In the foot fault test, IL-4 treatment still decreased forelimb and hindlimb foot fault rates in PPAR γ cKO mice after TBI (Figure 7(h) and (i)), but to a much lower extent than in WT mice (Figure 1). Moreover, IL-4 treatment showed no effect on gross brain tissue loss in PPAR γ cKO mice at 35 days after TBI (Figure S6(a) and (b)). These results demonstrate that IL-4 fails to promote white matter integrity when PPAR γ is not expressed in OPCs, resulting in weaker or no protection of neurological function.

Discussion

We demonstrated the robustly protective roles of IL-4 treatments after TBI in the present study, by examining histological, DTI, electrophysiological, and behavioral parameters. Despite its failure to prevent gross neuronal tissue loss, intranasal administration of IL-4 after TBI significantly promoted the structural and functional integrity of white matter in perilesional areas. Mechanistically, IL-4 facilitated OPC differentiation and oligodendrogenesis through PPAR γ activation, which enhanced white matter integrity and neurobehavioral recovery. The boost in white matter integrity with IL-4 likely contributed to the recovery of long-term sensorimotor functions. These results suggest a potential novel role for IL-4 in the protection of white matter and long-term functional recovery after TBI.

Traumatic brain injury is pathologically characterized by both gray and white matter injury, and for which there is currently no cure.³⁴ Here, we leveraged the intranasal route into the brain as direct means of drug delivery to the injured central nervous system.³⁵ Our findings that delayed IL-4 delivery improved long-term sensorimotor functions after TBI are consistent with our previous work on IL-4-mediated neuroprotection in experimental cerebral ischemia.^{11,13,15} Other studies have reported similarly beneficial effects of IL-4 upon neurological functions. For example, T cell-derived IL-4 is critical for memory and learning in the normal brain.³⁶ Second, the expression levels of IL-4 in the brain decrease with age, which may contribute to cognitive decline in aged populations.³⁷ We did not analyze cognitive function in the present study, but

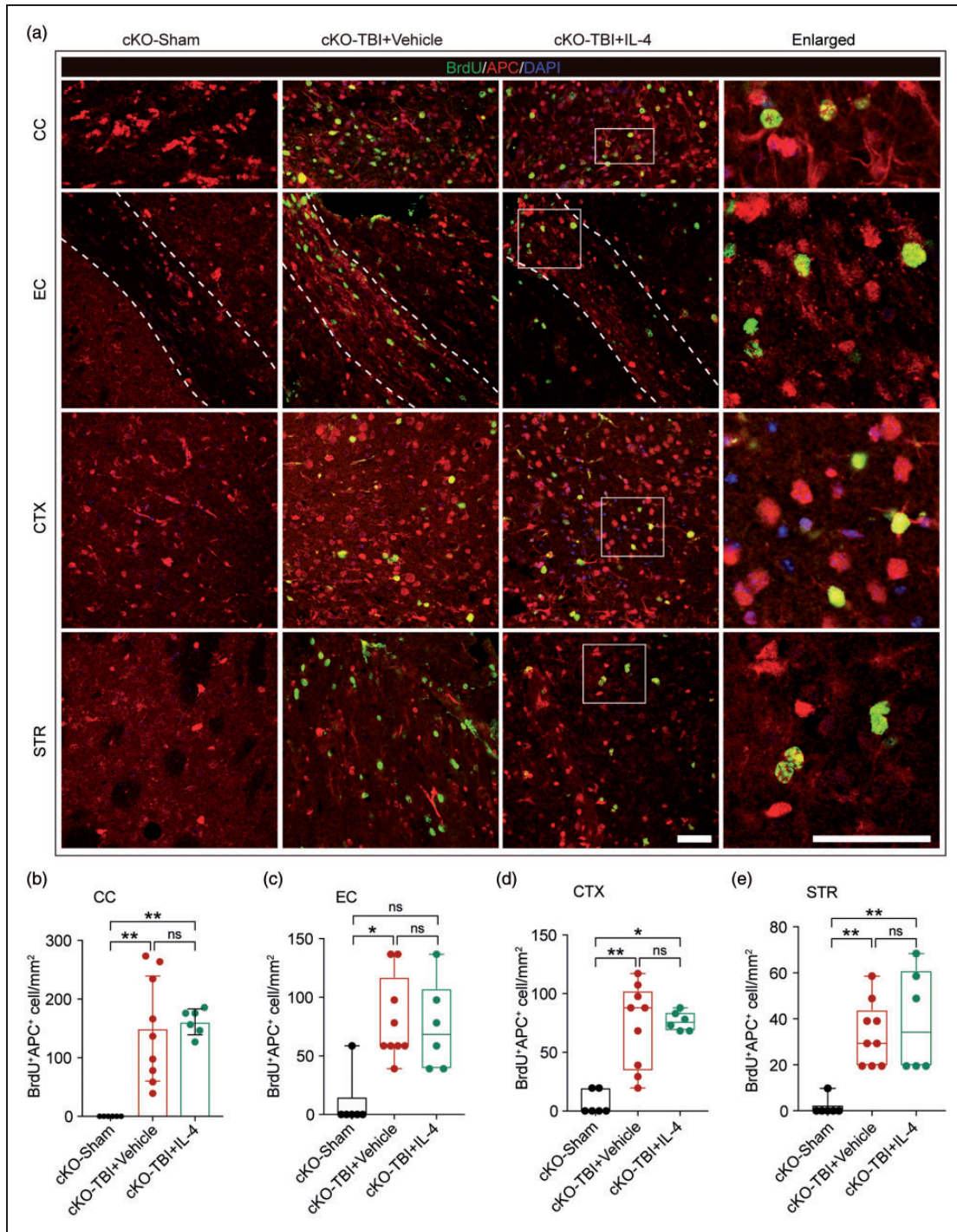


Figure 6. IL-4 treatment fails to enhance oligodendrogenesis in PPAR γ cKO mice after TBI. (a) Representative images showing BrdU and APC double immunostaining in the CC, EC, CTX, and STR in OPC-specific PPAR γ cKO mice at 35 days after TBI. Scale bar = 50 μ m. The dotted white lines trace the boundaries of the EC. (b–e) Quantification of BrdU⁺APC⁺ cells in the CC, EC, CTX, and STR. * p < 0.05, ** p < 0.01, ns: no significant difference, by one-way ANOVA followed by Bonferroni post hoc or Kruskal–Wallis test with Dunn post hoc. n = 6 in sham group, n = 9 in Vehicle group, n = 6 in IL-4 group.

future studies of the impact of IL-4 on cognitive functions in the context of TBI would be valuable.

Traumatic injury in white matter initiates numerous pathologies, including acute oligodendrocyte and

axonal injury as well as impaired axonal conduction between neural networks. Severe traumatic injury may gradually evolve into chronic, long-term white matter impairment, unless endogenous repair processes

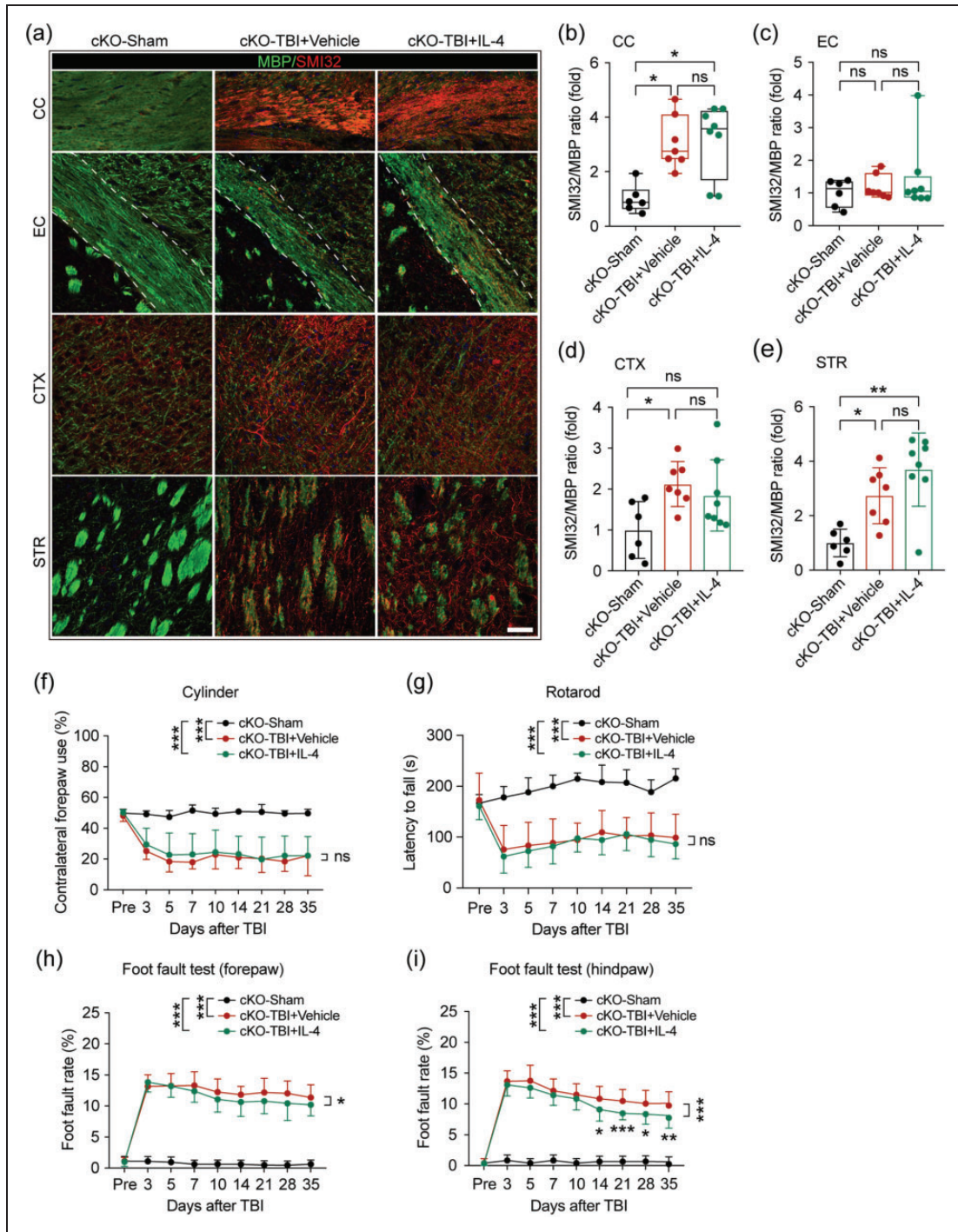


Figure 7. PPAR γ is essential for IL-4-induced structural improvements of white matter integrity and long-term neurological recovery after TBI. The impact of IL-4 treatment on white matter integrity was examined in PPAR γ cKO mice at 35 days after TBI. (a) Representative images of MBP and SMI32 double immunostaining in coronal brain sections of PPAR γ cKO mice at 35 days after TBI. Scale bar = 50 μ m. (b–e) Quantification of the SMI32/MBP ratio in the CC, EC, CTX, and STR areas. $n = 6$ in sham group, $n = 7$ in vehicle group, $n = 8$ in IL-4 group. * $p < 0.05$, ** $p < 0.01$, ns: no significant difference, by one-way ANOVA followed by Bonferroni post hoc or Kruskal–Wallis test with Dunn post hoc. (f) Asymmetry in contralateral forepaw use showed no difference between vehicle and IL-4-treated mice after OPC-specific PPAR γ KO. (g) The latency to fall in the rotarod test showed no difference between vehicle and IL-4-treated mice after OPC-specific PPAR γ KO. (h, i) The foot fault rates of forepaws (h) and hind paws (i) were evaluated by the foot fault test in PPAR γ cKO mice up to 35 days after TBI. * $p < 0.05$, ** $p < 0.01$, *** $p < 0.001$, ns: no significant difference, by two-way repeated measures ANOVA and Bonferroni post hoc tests. $n = 8$ in sham group, $n = 10$ in vehicle and IL-4-treated group in cylinder and rotarod test; $n = 8$ in sham group, $n = 17$ in vehicle and $n = 18$ IL-4-treated group in foot fault test.

are successfully activated.^{34,38,39} Consistent with our previous work,²² TBI induced both acute and chronic axonal injury, as demonstrated by accumulation of β -APP particles along neurofilaments at 3 days after TBI and decreased NF200 signal at 35 days after TBI. In addition, TBI disrupted myelin integrity, as evidenced by increases in the SMI32/MBP ratio, a measure that lies in proportion to the degree of oligodendrocyte injury and demyelination.

Brain injury is known to increase glial expression of IL-4-specific receptors, including on microglia/macrophage and oligodendrocyte lineage cells.¹¹ IL-4 is a well-known immune modulator and exerts direct or indirect roles in the regulation of white matter components in the CNS.^{15,40} A protective role of IL-4 against demyelination has been reported in experimental multiple sclerosis, in which IL-4 knockout mice suffer from increased demyelination and functional deficits.⁴¹ Furthermore, an *in vitro* study using mixed glial cultures demonstrated that IL-4 promotes the differentiation of OPCs into mature OLs by anti-inflammatory actions on astrocytes and microglia.⁴² The regeneration of myelin-forming OLs and the remyelination of functional axons are essential steps for the restoration of white matter integrity.⁴³ In addition to its well-known anti-inflammatory effects, our previous study identified a new function of IL-4 in the direct stimulation of OPC differentiation into mature OLs under conditions of brain ischemia.¹⁵ In the present study, we confirmed that IL-4 also promotes OPC differentiation *in vitro* and stimulates oligodendrogenesis in perilesional areas *in vivo* after TBI.

PPAR γ is a master transcription factor that could enhance myelin lipid synthesis, reduce oxidative stress, and promote mitochondrial function, thus promote OPC differentiation into mature OLs.⁴⁴ We previously reported that the PPAR γ agonist rosiglitazone promotes OPC proliferation and increases the generation of mature oligodendrocytes after brain ischemia.²³ In that study, we also showed that PPAR γ inhibition *in vitro* or OPC-specific PPAR γ KO *in vivo* attenuated the ability of IL-4 to enhance OPC differentiation and oligodendrocyte replacement after brain ischemia.¹⁵ PPAR γ agonists have been shown the abilities to inhibit inflammation,^{45,46} neurotoxicity,⁴⁷ neuronal autophagy, and apoptosis⁴⁸ after TBI. However, the role of PPAR γ in white matter function after TBI had not been addressed. Here, we have demonstrated that IL-4 improves OPC differentiation and oligodendrogenesis after TBI by activating PPAR γ signaling. Precisely how IL-4 binding to its receptor and activate PPAR γ is not yet examined, but IL-4 may activate PPAR γ via signal transducer and activator of transcription 6 (STAT6) in macrophages and other cell types according to previous studies.^{42,49} Whether IL-4 activate

PPAR γ through STAT6 in OPCs was not investigated in the present study but warrants further studies. In the present study, we did not find the impairment of spontaneous oligodendrogenesis with the conditional knockout of PPAR γ in OPCs. This may indicate that there is no endogenous compensatory increase in PPAR γ in OPCs after TBI. In different experimental settings and studies, the expression of PPAR γ in brains after TBI has been controversial. In a murine CCI model, no significant change of PPAR γ mRNA expression was found in the brain following TBI.^{50,51} On the contrary, Yi et al.⁴⁵ reported that the PPAR γ mRNA expression was increased by two folds at 24 h after experimental TBI. Another study detected clinical specimens and found that both the mRNA and protein level of PPAR γ were decreased in TBI patients.⁵² Future studies on how the endogenous IL-4 and PPAR γ changes in OPCs and OLs after TBI may be of value.

Consistent with its failure to enhance oligodendrogenesis after TBI in the absence of PPAR γ in OPCs, IL-4 also did not affect the SMI32/MBP ratio in OPC-specific PPAR γ KO mice. However, IL-4 treatment still decreased both forelimb and hind limb foot fault rates in PPAR γ KO mice, albeit to a lower extent than in WT mice. This result may be explained by the persistent anti-inflammatory functions of IL-4 and its regulation of microglia/macrophage polarization.^{53,54} In the present study, we did not analyze inflammatory cascades in the brain, but future studies to address this question may also be of value.

In conclusion, the present study demonstrates a novel therapeutic approach for TBI. Intranasal administration of IL-4 nanoparticles after TBI preserved the integrity of white matter and promoted long-term sensorimotor recovery. These protective effects may partly come from the promotion of OPC differentiation and oligodendrogenesis through PPAR γ . Overall, these results indicate that IL-4 might be leveraged as a promising therapeutic option for potential white matter restoration and functional neuroprotection after TBI.

Funding

The author(s) disclosed receipt of the following financial support for the research, authorship, and/or publication of this article: This work was supported by Merit Review grants from the US Department of Veterans Affairs (VA) (I01 BX003377) to JC; H.P. was supported by the American Heart Association Grant 17POST33661207. J.C. is the Richard King Mellon Professor of Neurology at the University of Pittsburgh and also supported by the Senior Research Career Scientist Award from the Department of Veterans Affairs. We thank Lesley M. Foley for technical

assistance with MRI experiments and Patricia Strickler for administrative support.





Declaration of conflicting interests

The author(s) declared no potential conflicts of interest concerning the research, authorship, and/or publication of this article.

Authors' contributions

HP, XZ, WZ, FX, YJ and HM performed experiments; XJ, HP, HM, TKH, QY, and WZ analyzed data; JC, XH, MVLB, and YS designed the study and supervised the project; HP, XJ wrote the manuscript; JC, CED, MVLB, and RKL interpreted the data and critically revised the manuscript.

ORCID iDs

Hongjian Pu  <https://orcid.org/0000-0001-5435-7070>
 Hongfeng Mu  <https://orcid.org/0000-0003-4444-9590>
 Yejie Shi  <https://orcid.org/0000-0001-7502-9201>
 Xiaoming Hu  <https://orcid.org/0000-0002-5857-6243>

Supplemental material

Supplemental material for this article is available online.

References

- Kinnunen KM, Greenwood R, Powell JH, et al. White matter damage and cognitive impairment after traumatic brain injury. *Brain* 2011; 134: 449–463.
- Wooten DW, Ortiz-Teran L, Zubcevic N, et al. Multimodal signatures of tau pathology, neuronal fiber integrity, and functional connectivity in traumatic brain injury. *J Neurotrauma* 2019; 36: 3233–3243
- Loane DJ and Faden AI. Neuroprotection for traumatic brain injury: translational challenges and emerging therapeutic strategies. *Trends Pharmacol Sci* 2010; 31: 596–604.
- Sidaros A, Engberg AW, Sidaros K, et al. Diffusion tensor imaging during recovery from severe traumatic brain injury and relation to clinical outcome: a longitudinal study. *Brain* 2008; 131: 559–572.
- Bigler ED. Distinguished neuropsychologist award lecture 1999. The lesion(s) in traumatic brain injury: implications for clinical neuropsychology. *Arch Clin Neuropsychol* 2001; 16: 95–131.
- Maxwell WL. Damage to myelin and oligodendrocytes: a role in chronic outcomes following traumatic brain injury? *Brain Sci* 2013; 3: 1374–1394.
- Hill CS, Coleman MP and Menon DK. Traumatic axonal injury: mechanisms and translational opportunities. *Trends Neurosci* 2016; 39: 311–324.
- Sullivan GM, Mierzwa AJ, Kijpaisalratana N, et al. Oligodendrocyte lineage and subventricular zone response to traumatic axonal injury in the corpus callosum. *J Neuropathol Exp Neurol* 2013; 72: 1106–1125.
- Segovia KN, McClure M, Moravec M, et al. Arrested oligodendrocyte lineage maturation in chronic perinatal white matter injury. *Ann Neurol* 2008; 63: 520–530.
- Gadani SP, Cronk JC, Norris GT, et al. Il-4 in the brain: a cytokine to remember. *J Immunol* 2012; 189: 4213–4219.
- Liu X, Liu J, Zhao S, et al. Interleukin-4 is essential for microglia/macrophage m2 polarization and long-term recovery after cerebral ischemia. *Stroke* 2016; 47: 498–504.
- Ting SM, Zhao X, Zheng X, et al. Excitatory pathway engaging glutamate, calcineurin, and NFAT upregulates il-4 in ischemic neurons to polarize microglia. *J Cereb Blood Flow Metab* 2020; 40: 513–527.
- Xiong X, Barreto GE, Xu L, et al. Increased brain injury and worsened neurological outcome in interleukin-4 knockout mice after transient focal cerebral ischemia. *Stroke* 2011; 42: 2026–2032.
- Yoshizaki K, Adachi K, Kataoka S, et al. Chronic cerebral hypoperfusion induced by right unilateral common carotid artery occlusion causes delayed white matter lesions and cognitive impairment in adult mice. *Exp Neurol* 2008; 210: 585–591.
- Zhang Q, Zhu W, Xu F, et al. The interleukin-4/PPARgamma signaling axis promotes oligodendrocyte differentiation and remyelination after brain injury. *PLoS Biol* 2019; 17: e3000330.
- National Research Council. *Guide for the care and use of laboratory animals*. 8th ed. Washington, DC: National Academies Press, 2011.
- Kang SH, Fukaya M, Yang JK, et al. Ng2+ CNS glial progenitors remain committed to the oligodendrocyte lineage in postnatal life and following neurodegeneration. *Neuron* 2010; 68: 668–681.
- Wang G, Shi Y, Jiang X, et al. HDAC inhibition prevents white matter injury by modulating microglia/macrophage polarization through the GSK3beta/PTEN/Akt axis. *Proc Natl Acad Sci U S A* 2015; 112: 2853–2858.
- Zhang J, Zhang W, Gao X, et al. Preconditioning with partial caloric restriction confers long-term protection against grey and white matter injury after transient focal ischemia. *J Cereb Blood Flow Metab* 2019; 39: 1394–1409.
- Zhang J, Pu H, Zhang H, et al. Inhibition of na(+)-k(+)-2cl(-) cotransporter attenuates blood-brain-barrier disruption in a mouse model of traumatic brain injury. *Neurochem Int* 2017; 111: 23–31.
- Dai X, Chen J, Xu F, et al. TGFalpha preserves oligodendrocyte lineage cells and improves white matter integrity after cerebral ischemia. *J Cereb Blood Flow Metab* 2020; 40: 639–655.
- Xia Y, Pu H, Leak RK, et al. Tissue plasminogen activator promotes white matter integrity and functional recovery in a murine model of traumatic brain injury. *Proc Natl Acad Sci U S A* 2018; 115: E9230–E9238.
- Han L, Cai W, Mao L, et al. Rosiglitazone promotes white matter integrity and long-term functional recovery after focal cerebral ischemia. *Stroke* 2015; 46: 2628–2636.

24. Jiang X, Suenaga J, Pu H, et al. Post-stroke administration of omega-3 polyunsaturated fatty acids promotes neurovascular restoration after ischemic stroke in mice: efficacy declines with aging. *Neurobiol Dis* 2019; 126: 62–75.
25. Wilde EA, McCauley SR, Kelly TM, et al. The neurological outcome scale for traumatic brain injury (NOS-TBI): I. Construct validity. *J Neurotrauma* 2010; 27: 983–989.
26. Hellewell SC, Yan EB, Alwis DS, et al. Erythropoietin improves motor and cognitive deficit, axonal pathology, and neuroinflammation in a combined model of diffuse traumatic brain injury and hypoxia, in association with upregulation of the erythropoietin receptor. *J Neuroinflammation* 2013; 10: 156.
27. Alexander AL, Lee JE, Lazar M, et al. Diffusion tensor imaging of the brain. *Neurotherapeutics* 2007; 4: 316–329.
28. Monje M. Myelin plasticity and nervous system function. *Annu Rev Neurosci* 2018; 41: 61–76.
29. Keough MB, Rogers JA, Zhang P, et al. An inhibitor of chondroitin sulfate proteoglycan synthesis promotes central nervous system remyelination. *Nat Commun* 2016; 7: 11312.
30. Kato M, Nagaya T, Fujieda M, et al. Expression of PPARgamma and its ligand-dependent growth inhibition in human brain tumor cell lines. *Jpn J Cancer Res* 2002; 93: 660–666.
31. Bernardo A, De Simone R, De Nuccio C, et al. The nuclear receptor peroxisome proliferator-activated receptor-gamma promotes oligodendrocyte differentiation through mechanisms involving mitochondria and oscillatory Ca^{2+} waves. *Biol Chem* 2013; 394: 1607–1614.
32. Saluja I, Granneman JG and Skoff RP. PPAR delta agonists stimulate oligodendrocyte differentiation in tissue culture. *Glia* 2001; 33: 191–204.
33. Bernardo A, Giammarco ML, De Nuccio C, et al. Docosahexaenoic acid promotes oligodendrocyte differentiation via PPAR-gamma signalling and prevents tumor necrosis factor-alpha-dependent maturational arrest. *Biochim Biophys Acta Mol Cell Biol Lipids* 2017; 1862: 1013–1023.
34. Armstrong RC, Mierzwa AJ, Sullivan GM, et al. Myelin and oligodendrocyte lineage cells in white matter pathology and plasticity after traumatic brain injury. *Neuropharmacology* 2016; 110: 654–659.
35. Alshweiat A, Ambrus R and Csoka I. Intranasal nanoparticulate systems as alternative route of drug delivery. *Curr Med Chem* 2019; 26: 6459–6492.
36. Derecki NC, Cardani AN, Yang CH, et al. Regulation of learning and memory by meningeal immunity: a key role for il-4. *J Exp Med* 2010; 207: 1067–1080.
37. Nolan Y, Maher FO, Martin DS, et al. Role of interleukin-4 in regulation of age-related inflammatory changes in the hippocampus. *J Biol Chem* 2005; 280: 9354–9362.
38. Armstrong RC, Mierzwa AJ, Marion CM, et al. White matter involvement after TBI: clues to axon and myelin repair capacity. *Exp Neurol* 2016; 275(Pt 3): 328–333.
39. Marion CM, Radomski KL, Cramer NP, et al. Experimental traumatic brain injury identifies distinct early and late phase axonal conduction deficits of white matter pathophysiology, and reveals intervening recovery. *J Neurosci* 2018; 38: 8723–8736.
40. van Wageningen TA, Vlaar E, Kooij G, et al. Regulation of microglial tmem119 and P2RY12 immunoreactivity in multiple sclerosis white and grey matter lesions is dependent on their inflammatory environment. *Acta Neuropathol Commun* 2019; 7: 206.
41. Falcone M, Rajan AJ, Bloom BR, et al. A critical role for IL-4 in regulating disease severity in experimental allergic encephalomyelitis as demonstrated in IL-4-deficient c57BL/6 mice and BALB/C mice. *J Immunol* 1998; 160: 4822–4830.
42. Paintlia AS, Paintlia MK, Singh I, et al. Il-4-induced peroxisome proliferator-activated receptor gamma activation inhibits NF-kappaB trans activation in central nervous system (CNS) glial cells and protects oligodendrocyte progenitors under neuroinflammatory disease conditions: implication for CNS-demyelinating diseases. *J Immunol* 2006; 176: 4385–4398.
43. Franklin RJM and ffrench-Constant C. Regenerating CNS myelin – from mechanisms to experimental medicines. *Nat Rev Neurosci* 2017; 18: 753–769.
44. Cai W, Yang T, Liu H, et al. Peroxisome proliferator-activated receptor gamma (PPARgamma): a master gatekeeper in CNS injury and repair. *Prog Neurobiol* 2018; 163–164: 27–58.
45. Yi JH, Park SW, Brooks N, et al. PPARgamma agonist rosiglitazone is neuroprotective after traumatic brain injury via anti-inflammatory and anti-oxidative mechanisms. *Brain Res* 2008; 1244: 164–172.
46. Liu H, Rose ME, Culver S, et al. Rosiglitazone attenuates inflammation and Ca^{3+} neuronal loss following traumatic brain injury in rats. *Biochem Biophys Res Commun* 2016; 472: 648–655.
47. He J, Liu H, Zhong J, et al. Bexarotene protects against neurotoxicity partially through a PPARgamma-dependent mechanism in mice following traumatic brain injury. *Neurobiol Dis* 2018; 117: 114–124.
48. Yao J, Zheng K and Zhang X. Rosiglitazone exerts neuroprotective effects via the suppression of neuronal autophagy and apoptosis in the cortex following traumatic brain injury. *Mol Med Rep* 2015; 12: 6591–6597.
49. Szanto A, Balint BL, Nagy ZS, et al. Stat6 transcription factor is a facilitator of the nuclear receptor PPARgamma-regulated gene expression in macrophages and dendritic cells. *Immunity* 2010; 33: 699–712.
50. Thal SC, Wyschkon S, Pieter D, et al. Selection of endogenous control genes for normalization of gene expression analysis after experimental brain trauma in mice. *J Neurotrauma* 2008; 25: 785–794.
51. Thal SC, Heinemann M, Luh C, et al. Pioglitazone reduces secondary brain damage after experimental brain trauma by PPAR-gamma-independent mechanisms. *J Neurotrauma* 2011; 28: 983–993.
52. Deng Y, Jiang X, Deng X, et al. Pioglitazone ameliorates neuronal damage after traumatic brain injury via the

- PPAR γ /NF- κ B/IL-6 signaling pathway. *Gene Dis* 2020; 7: 253–265.
53. Francos-Quijorna I, Amo-Aparicio J, Martinez-Muriana A, et al. Il-4 drives microglia and macrophages toward a phenotype conducive for tissue repair and functional recovery after spinal cord injury. *Glia* 2016; 64: 2079–2092.
54. Chao CC, Molitor TW and Hu S. Neuroprotective role of il-4 against activated microglia. *J Immunol* 1993; 151: 1473–1481.